analyzing powers for the $5/2^-$ transition are more positive than for the strong $7/2^-$ and $3/2^-$. The second $7/2^-$ state is weak and may not proceed in one step.

One striking result is that the rainbow mechanism has less influence on A_{yy}, so that this analyzing power shows stronger variations with structure. This result is consistent with the observation of small tensor analyzing powers in the continuum (reported in a separate contribution to this report). It may thus be worthwhile to investigate more thoroughly the use of tensor analyzing powers to extract structure information. This may provide in some cases particularly clean signals, as has been recently noted for $(\vec{d},\alpha)$ reactions at lower energies.[7)]

5. Other Rainbow Projectiles. The spin dependence of rainbow scattering was first observed for deuterons because of the availability of polarized beams of intermediate energies. However, rainbow effects are common in the scattering of helium and lithium isotopes. So it is clear that strong saturation of the analyzing powers will be observed there as well at energies in excess of 25 MeV/A. This should be especially true for ^{3}He and ^{3}H, where the spin-orbit potential is already known to exceed the expectations of a simple folding-model prescription.

At the same time, proton elastic scattering exhibits large, positive values of the vector analyzing power while the cross section exhibits a diffractive pattern at all angles. In an optical-model calculation, the features of rainbow scattering (a large-angle cross section enhancement followed by a smooth exponential decline with angle) can be recovered by reducing the strength of the imaginary potential. Increasing the strength quickly drives the analyzing powers to near zero. Thus the positive-going rise in the analyzing power may be interpreted as a remnant of rainbow scattering, which is almost extinguished by the imaginary part of the proton-nucleus interaction.

1) E.J. Stephenson, C.C. Foster, P. Schwandt, and D.A. Goldberg, to be published in Nucl. Phys.

2) R.C. Johnson and E.J. Stephenson, to be published.

3) G. Perrin, Nguyen van Sen, J. Arvieux, R. Darves-Blanc, J.L. Durand, A. Fiore, J.C. Gondrand, F. Merchez, and C. Perrin, Nucl. Phys. A282, 221 (1977).

4) A.A. Ioannides and R.C. Johnson, Phys. Rev. C17, 1331 (1978).

5) R.P. Goddard, Nucl. Phys. A291, 13 (1977).

6) F. Seiler, F.N. Rad, H.E. Conzett, and R. Roy, Nucl. Phys. A296, 205 (1978).

7) S.A. Tonsfeldt, T.B. Clegg, E.J Ludwig, Y. Tagishi, and J.F. Wilkerson, Phys. Rev. Lett. 45, 2008 (1980).

ELASTIC SCATTERING OF 178 MeV ALPHA PARTICLES FROM ^{58}Ni AND ^{208}Pb

W.D. Ploughe and J.W. Kerns
The Ohio State University, Columbus, Ohio 43212

W.W. Jacobs and P. Schwandt
Indiana University Cyclotron Facility, Bloomington, Indiana 47405

The differential cross sections for elastic scattering of 178 MeV alpha particles from ^{58}Ni and ^{208}Pb were measured using the QDDM spectrograph. Isotopically enriched targets of ^{58}Ni (thickness 8 and 28 mg/cm^2) and ^{208}Pb (12 mg/cm^2) were used. Over the angular range $8° < \theta_{lab} < 70°$ covered, the measured cross sections span over eight orders of magnitude.

Initial attempts to reproduce the data with a phenomenological optical-model potential taken from the literature are shown in Figs. 1 and 2. The curves

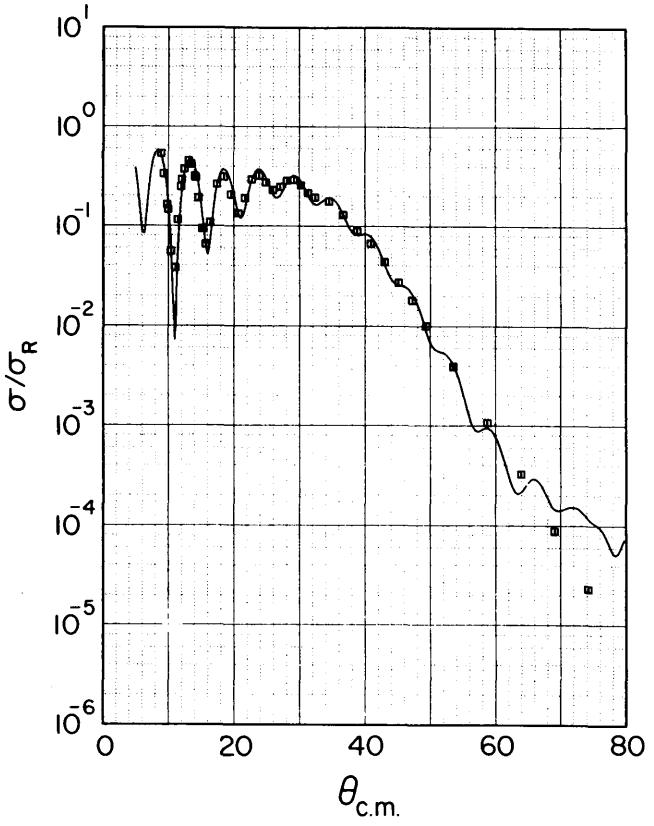

Figure 1. Angular distribution of the differential cross section for α + ^{58}Ni at 178 MeV normalized to Rutherford scattering. The curve is an optical-model calculation using the 166 MeV parameters of Bimbot et al. (Table 1).

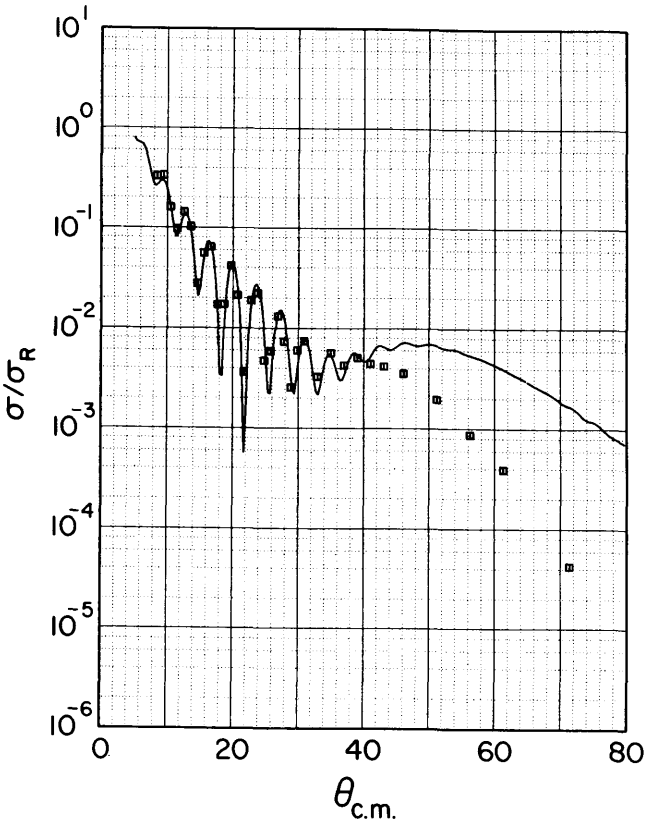

Figure 2. Angular distribution of the differential cross section for α + ^{208}Pb at 178 MeV normalized to Rutherford scattering. The curve is an optical-model calculation using the 166 MeV parameters of Bimbot et al. (Table 1).

shown were calculated using the parameters of Bimbot et al.[1] for 166 MeV alpha scattering; these parameters are reproduced here in Table 1. The angular distribution for ^{58}Ni is quite well fitted for angles up to 60° but somewhat overpredicted by the optical model at larger angles, while for ^{208}Pb the calculation exceeds the measurements considerably for angles greater than 40° (in all cases the data errors are smaller than the size of the data points shown in the figures, except for the θ_{lab} = 70° points where the error is about ± 20%).

The fit to the present ^{58}Ni data using the Bimbot potential parameters (Table 1) is surprisingly good, considering that the 166 MeV measurements apparently do not extend beyond 35° (as shown in ref. 2). We shall pursue the analysis of both sets of 178 MeV data in order to elucidate the extent to which the large-angle data constrain the standard optical-model parametrization. In addition, potential form factors other than the customary Woods-Saxon shape and semi-microscopic potential models will be explored.

Table 1. Phenomenological optical-model parameters [from Bimbot et al.[1]] used for an initial fit to the data shown in Figures 1 and 2. (Potential strengths in MeV, geometry parameters in fm)

	V	RO	AO	W	RW	AW
^{58}Ni	107.4	1.27	0.75	22.6	1.59	0.50
^{208}Pb	119.9	1.26	0.74	21.3	1.45	0.80

1) L. Bimbot, B. Tatischeff, I. Brissaud, Y. Le Bornec, N. Frascaria, and A. Willis, Nucl. Phys. A210, 397 (1973).

2) J. Van de Wiele, E. Gerlic, H. Langevin-Joliot, and G. DuHamel, Nucl. Phys. A297, 61 (1978).